Pramana – J. Phys. (2017) 89:67
DOI 10.1007/s12043-017-1464-2

Exploring a hidden fermionic dark sector

DEBASISH MAJUMDAR[1,*], AMIT DUTTA BANIK[1] and ANIRBAN BISWAS[2]

[1]Saha Institute of Nuclear Physics, HBNI, 1/AF, Bidhannagar, Kolkata 700 064, India
[2]Harish-Chandra Research Institute, Jhusi, Allahabad 211 019, India
*Corresponding author. E-mail: debasish.majumdar@saha.ac.in

Published online 9 October 2017

Abstract. We propose a hidden sector fermion dark matter model which follows a dark $SU(2)_{\rm H}$ symmetry. Fermions in the dark sector also carry a global $U(1)_{\rm H}$ charge while the gauge bosons and dark scalar do not have any global $U(1)_{\rm H}$ charge. The lightest fermion in dark sector can serve as a potential dark matter candidate. We investigate whether the proposed dark matter candidate can explain indirect detection results from galactic centre.

Keywords. Dark matter; γ-ray flux; hidden sector.

PACS Nos 12.60.Jv; 12.10.Dm; 98.80.Cq; 11.30.Hv

1. Introduction

Study of temperature anisotropy in cosmic microwave background radiation (CMBR) by Planck [1] satellite experiment suggests that about 25% of the Universe is made up of dark matter. Observations of gravitational lensing effects from galactic centre and rotation curves of spiral galaxies also provide strong evidence for dark matter (DM). However, the nature of dark matter and its particle constituent remain unknown. Standard Model (SM) of particle physics also cannot explain the physics of dark matter. Different particle physics models for dark matter are proposed to provide a viable candidate for DM where stability of dark matter is ensured by a discrete symmetry [2–17]. Apart from that, there are also models for dark matter with continuous symmetry [18–23]. In this work, we present a hidden sector model for dark matter without imposing any such discrete symmetry. Dark matter in the hidden sector can interact with particles in the SM via scalar bosons. We also test the viability of such dark matter candidates with experimental limits from direct detection experiments such as LUX [24] and also with indirect detection results obtained from the study of γ-ray flux at the galactic centre (GC). The paper is organized as follows. In §2, detailed study of the proposed hidden sector dark matter model is presented. In the next section the constraints on the model from Large Hadron Collider (LHC) and bounds of invisible decay are mentioned. In §4, the thermal evolution and Boltzmann equation for the dark matter candidate are described. The results from direct and indirect detections of dark matter are shown in §5. Finally, the paper is summarized with concluding remarks.

2. Hidden sector dark matter model

We invoke a hidden sector dark matter model where the hidden sector or dark sector is invariant under a dark local $SU(2)_{\rm H}$ symmetry and a global $U(1)_{\rm H}$ symmetry. While the fermions in the dark sector are invariant under local $SU(2)_{\rm H}$ and global $U(1)_{\rm H}$, the scalar doublet follows only the local $SU(2)_{\rm H}$. According to Witten anomaly [25], such a model would survive only with even number of fermion generations. Hence, we consider two fermion generations χ_i $(i = 1,\ 2)$ each having two fermions resulting in four fermions f_i $(i = 1, 4)$. Similar to SM, here also left-handed fermion transforms as $SU(2)_{\rm H}$ while right-handed fermions are singlet under $SU(2)_{\rm H}$. After spontaneous symmetry breaking (SSB), the scalar doublet Φ develops a vacuum expectation value v_s. It is to be noted that as the scalar doublet does not have any global $U(1)_{\rm H}$ charge, this symmetry remains unbroken. Also gauge bosons in the dark sector $A'_{i\,\mu}$ $(i = 1$–$3)$ acquire mass due to the breaking of this local $SU(2)_{\rm H}$ and they are mass degenerate. Fermions in the dark sector also achieve mass from the spontaneous breaking of this $SU(2)_{\rm H}$ via dark Higgs doublet Φ. We assume the gauge bosons $A'_{i\,\mu}$ $(i = 1$–$3)$ to be heavier than the fermions. Therefore, lightest fermion in dark

sector can serve as a potential candidate for dark matter assuming these fermions are in mass basis or following CKM, two of the fermions are in their mass basis (f_1, f_3) and other two (f_2, f_4) mix with each other. In both cases mentioned above, we assume f_1, the lightest of all fermions with mass m_{f_1}, is the potential DM candidate. The total Lagrangian for the hidden sector dark matter model as stated above can be expressed as

$$\begin{aligned}\mathcal{L} \supset & -\frac{1}{4}F'_{\mu\nu}F'^{\mu\nu} + (D_\mu H)^\dagger (D^\mu H) \\ & + (D'_\mu \Phi)^\dagger (D'^\mu \Phi) - \mu_1^2\, H^\dagger H - \mu_2^2\, \Phi^\dagger \Phi \\ & - \lambda_1 (H^\dagger H)^2 - \lambda_2 (\Phi^\dagger \Phi)^2 - \lambda_3\, H^\dagger H \Phi^\dagger \Phi \\ & + \sum_{i=1,2} \bar{\chi}_{i\mathrm{L}} (i \not{D}' \chi_{i\mathrm{L}}) + \sum_{i=1,4} \bar{f}_{i\mathrm{R}} (i \not{\partial} f_{i\mathrm{R}}) \\ & - y'_1\, \bar{\chi}_{1\mathrm{L}}\, \Phi f_{1\mathrm{R}} - y'_2\, \bar{\chi}_{1\mathrm{L}}\, \tilde{\Phi} f_{2\mathrm{R}}, \\ & - y'_3\, \bar{\chi}_{2\mathrm{L}}\, \Phi f_{3\mathrm{R}} - y'_4\, \bar{\chi}_{2\mathrm{L}}\, \tilde{\Phi} f_{4\mathrm{R}} + \mathrm{h.c.}, \end{aligned} \tag{1}$$

where

$$H = \begin{pmatrix} G_1^+ \\ \frac{h^0 + iG_1^0}{\sqrt{2}} \end{pmatrix}, \quad \Phi = \begin{pmatrix} G_2^+ \\ \frac{\phi^0 + iG_2^0}{\sqrt{2}} \end{pmatrix},$$

$$\chi_{1\mathrm{L}} = \begin{pmatrix} f_1 \\ f_2 \end{pmatrix}_{\mathrm{L}}, \quad \chi_{2\mathrm{L}} = \begin{pmatrix} f_3 \\ f_4 \end{pmatrix}_{\mathrm{L}}, \tag{2}$$

and covariant derivatives can be written as

$$D_\mu = \left(\partial_\mu + i\frac{g}{2} \sum_{a=1,3} \sigma_a W^a{}_\mu + i\frac{g'}{2} B_\mu \right),$$

$$D'_\mu = \left(\partial_\mu + i\frac{g_{\mathrm{H}}}{2} \sum_{a=1,3} \sigma^a A'_{a\,\mu} \right). \tag{3}$$

As mentioned earlier, masses of dark fermions are generated via SSB mechanism and therefore mass of the lightest fermion is $m_{f_1} = y'_1 v_s/\sqrt{2}$. For simplicity, we redefine mass of f_1 to be m. From eq. (1) it can be seen that the SM scalar doublet H can have mixing with hidden sector dark doublet field Φ. Hence, fermions in the dark sector can also interact with SM sector via scalar-mediated processes. The mixing between the SM Higgs doublet and dark Higgs doublet results in two physical scalars which can be expressed as

$$h_1 = \cos\alpha h^0 - \sin\alpha \phi^0, \quad h_2 = \sin\alpha h^0 + \cos\alpha \phi^0$$

with mixing angle

$$\alpha = \frac{1}{2}\, \tan^{-1}\left(\frac{(\lambda_3/\lambda_2)(v/v_s)}{1 - (\lambda_1/\lambda_2)(v^2/v_s^2)} \right). \tag{4}$$

Masses of these physical scalars h_i, $i = 1, 2$ are given as follows:

$$m_1 = \sqrt{\lambda_1 v^2 + \lambda_2 v_s^2 + \sqrt{(\lambda_1 v^2 - \lambda_2 v_s^2)^2 + (\lambda_3 v v_s)^2}}\,,$$

$$m_2 = \sqrt{\lambda_1 v^2 + \lambda_2 v_s^2 - \sqrt{(\lambda_1 v^2 - \lambda_2 v_s^2)^2 + (\lambda_3 v v_s)^2}}.$$

Here we assume that one of the physical scalars h_1 is an SM-like scalar having ∼125 GeV mass as obtained from LHC experiments (ATLAS [26] and CMS [27]) while the other scalar h_2 is presumed be dark scalar or non-SM scalar. It is to be noted that the scalar potential for the Lagrangian in eq. (1) must be bounded from below and stable. The conditions for vacuum stability in the above model is given as

$$\lambda_1 > 0, \quad \lambda_2 > 0\,, \quad \lambda_3 + 2\sqrt{\lambda_1 \lambda_2} > 0. \tag{5}$$

3. LHC phenomenology

Discovery of Higgs-like scalar at LHC of mass ∼125 GeV has been reported by ATLAS [26] and CMS [27]. ATLAS and CMS also provide the measure of signal strength of the Higgs-like scalar into different final-state pair of fermion– antifermion, gauge bosons or diphoton. As we have mentioned, the present model with hidden sector dark matter has two scalar bosons. In this work, we consider h_1 as SM-like scalar having mass $m_1 = 125$ GeV and h_2 as non-SM scalar. Signal strength for scalar bosons h_1 and h_2 can be given in the form

$$\begin{aligned} R_1 &= \frac{\sigma(pp \to h_1)}{\sigma^{\mathrm{SM}}(pp \to h)} \frac{\mathrm{Br}(h_1 \to xx)}{\mathrm{Br}^{\mathrm{SM}}(h \to xx)}, \\ R_2 &= \frac{\sigma(pp \to h_2)}{\sigma^{\mathrm{SM}}(pp \to h)} \frac{\mathrm{Br}(h_2 \to xx)}{\mathrm{Br}^{\mathrm{SM}}(h \to xx)}\,, \end{aligned} \tag{6}$$

where $\sigma(pp \to h_i)$, $i = 1, 2$ denotes the production cross-section of the scalar h_i and $\mathrm{Br}(h_i \to xx)$, $i = 1, 2$ is the respective branching ratio to any particular channel. In eq. (6), $\sigma^{\mathrm{SM}}(pp \to h)$ is the corresponding SM Higgs production cross-section with mass m_i while $\mathrm{Br}^{\mathrm{SM}}(h \to xx)$ is the measure of SM Higgs branching ratio with mass m_i. Branching ratios for h_i, $i = 1, 2$ into any specific channel is defined as

$$\mathrm{Br}(h_i \to xx) = \frac{\Gamma_i(h_i \to xx)}{\Gamma_i}, \tag{7}$$

where $\Gamma_i(h_i \to xx)$ is the decay width of h_i for xx final state while Γ_i gives the total decay width of h_i. Using the above expressions one can write

$$R_1 = \cos^4\alpha \frac{\Gamma^{\mathrm{SM}}}{\Gamma_1},$$

$$R_2 = \sin^4\alpha \frac{\Gamma^{\rm SM}}{\Gamma_2}, \tag{8}$$

where $\Gamma^{\rm SM}$ is the total decay witdh of the SM Higgs with mass m_1 (m_2) for signal strength R_1 (R_2). Expressions of Γ_1 and Γ_2 are given as

$$\Gamma_1 = \cos^2\alpha\Gamma^{\rm SM} + \Gamma_1^{\rm inv},$$
$$\Gamma_2 = \sin^2\alpha\Gamma^{\rm SM} + \Gamma_2^{\rm inv}. \tag{9}$$

$\Gamma_i^{\rm inv}$, $i = 1, 2$ denotes the invisible decay width of scalar h_i into dark matter pair which can be written as

$$\Gamma_1^{\rm inv} = \frac{m_1}{8\pi}\frac{m^2}{v_s^2}\sin^2\alpha\left(1-\frac{4m^2}{m_1^2}\right)^{3/2},$$
$$\Gamma_2^{\rm inv} = \frac{m_2}{8\pi}\frac{m^2}{v_s^2}\cos^2\alpha\left(1-\frac{4m^2}{m_2^2}\right)^{3/2}, \tag{10}$$

where v_s is the VEV of dark doublet and m is the mass of dark matter as mentioned in §2. As in the present work h_1 is the SM-like scalar (as $m_1 = 125$ eV), we consider $R_1 > 0.8$ [28] and branching ratio to invisible channel to be $\mathrm{Br}_{\rm inv}^1 \leq 0.2$ [29], is consistent with the findings from LHC.

4. Relic density and Boltzmann equation for dark matter

Relic abundance of dark matter obtained by Planck [1] is

$$\Omega_{\rm DM}h^2 = 0.1199 \pm 0.0027, \tag{11}$$

where Hubble parameter h is expressed in the unit of 100 km s^{-1} Mpc^{-1}. Dark matter relic abundance obtained from the solution of Boltzmann equation for the dark matter candidate is expressed as [30]

$$\frac{{\rm d}n}{{\rm d}t} + 3Hn = -\langle\sigma v\rangle(n^2 - n_{\rm eq}^2), \tag{12}$$

where $\langle\sigma v\rangle$ is the thermally averaged annihilation cross-section of dark matter. In eq. (12), the number density of the dark matter particle is written as n and its equilibrium number density is $n_{\rm eq}$. As the Universe expands, dark matter particles cool down and get decoupled from the thermal equilibrium of the Universe and freeze out. Relic density of dark matter after freeze-out is given as

$$\Omega_{\rm DM}h^2 = \frac{1.07\times10^9 x_f}{\sqrt{g_*}M_{\rm Pl}\langle\sigma v\rangle}, \tag{13}$$

where $x_f = m/T_{\rm F}$, $T_{\rm F}$ is the freeze-out temperature, $M_{\rm Pl} = 1.22\times10^{19}$ GeV is the Planck mass and g_* is the number of effective degrees of freedom (d.o.f.). Freeze-out temperature $T_{\rm F}$ can be obtained from iterative solution of the equation

$$x_f = \ln\left(\frac{m}{2\pi^3}\sqrt{\frac{45M_{\rm Pl}^2}{2g_*x_f}}\langle\sigma v\rangle\right). \tag{14}$$

Expressions for dark matter pair annihilation cross-section into different final-state fermion–antifermion pair is given as

$$\sigma v_{f\bar f} = N_c\frac{m^2}{v_s^2}\frac{s_\alpha^2c_\alpha^2}{8\pi}\frac{m_f^2}{v^2}\beta_f^{3/2}F(s),$$
$$\sigma v_{WW} = \frac{m^2}{v_s^2}\frac{s_\alpha^2c_\alpha^2}{8\pi s}\beta_W^{1/2}\left(\frac{2m_W^2}{v}\right)^2 \times\left(1+\frac{(s/2-m_W^2)^2}{2m_W^4}\right)F(s),$$
$$\sigma v_{ZZ} = \frac{m^2}{v_s^2}\frac{s_\alpha^2c_\alpha^2}{16\pi s}\beta_Z^{1/2}\left(\frac{2m_Z^2}{v}\right)^2 \times\left(1+\frac{(s/2-m_Z^2)^2}{2m_Z^4}\right)F(s), \tag{15}$$

where

$$F(s) = (s-4m^2) \times\left[\frac{1}{(s-m_1^2)^2+m_1^2\Gamma_1^2}+\frac{1}{(s-m_2^2)^2+m_2^2\Gamma_2^2} -\frac{2(s-m_1^2)(s-m_2^2)+2m_1m_2\Gamma_1\Gamma_2}{[(s-m_1^2)^2+m_1^2\Gamma_1^2][(s-m_1^2)^2+m_1^2\Gamma_2^2]}\right]$$

and $\beta_x = (1-(4m_x^2/s))$, $x = f, W, Z$. In eq. (14) s_α (c_α) denotes $\sin\alpha$ ($\cos\alpha$), s is the centre of momentum energy and N_c is the degeneracy factor due to colour quantum number (1 for leptons and 3 for quarks). Similarly, expressions for dark matter annihilation into scalar particles h_1 and h_2 are given as

$$\sigma v_{h_1h_1} = \frac{1}{16\pi s}\frac{m^2}{v_s^2}\left(1-\frac{4m_1^2}{s}+\frac{4m_1^2(m_1^2-1)}{s^2}\right)^{1/2} \times(s-4m^2)F'(s) \tag{16}$$

and

$$\sigma v_{h_2h_2} = \frac{1}{16\pi s}\frac{m^2}{v_s^2}\left(1-\frac{4m_2^2}{s}+\frac{4m_2^2(m_2^2-1)}{s^2}\right)^{1/2} \times(s-4m^2)F''(s), \tag{17}$$

where

$$F'(s) = \left[\frac{s_\alpha^2 \lambda_{111}^2}{(s-m_1^2)^2 + m_1^2\Gamma_1^2} + \frac{c_\alpha^2 \lambda_{211}^2}{(s-m_2^2)^2 + m_2^2\Gamma_2^2} - \frac{2 s_\alpha c_\alpha \lambda_{111}\lambda_{211}((s-m_1^2)(s-m_2^2) + 2m_1 m_2 \Gamma_1\Gamma_2)}{[(s-m_1^2)^2 + m_1^2\Gamma_1^2][(s-m_1^2)^2 + m_1^2\Gamma_2^2]} \right]$$

and

$$F''(s) = \left[\frac{s_\alpha^2 \lambda_{122}^2}{(s-m_1^2)^2 + m_1^2\Gamma_1^2} + \frac{c_\alpha^2 \lambda_{222}^2}{(s-m_2^2)^2 + m_2^2\Gamma_2^2} - \frac{2 s_\alpha c_\alpha \lambda_{122}\lambda_{222}((s-m_1^2)(s-m_2^2) + 2m_1 m_2 \Gamma_1\Gamma_2)}{[(s-m_1^2)^2 + m_1^2\Gamma_1^2][(s-m_1^2)^2 + m_1^2\Gamma_2^2]} \right].$$

Expression of the couplings in $F'(s)$ and $F''(s)$ are

$$\lambda_{111} = \lambda_1 v c_\alpha^3 - \lambda_2 v_s s_\alpha^3 + \frac{1}{2}\lambda_3 (v c_\alpha s_\alpha^2 - v_s s_\alpha c_\alpha^2),$$

$$\lambda_{222} = \lambda_1 v s_\alpha^3 + \lambda_2 v_s c_\alpha^3 + \frac{1}{2}\lambda_3 (v s_\alpha c_\alpha^2 + v_s c_\alpha s_\alpha^2),$$

$$\lambda_{211} = 3(\lambda_1 v c_\alpha^2 s_\alpha - \lambda_2 v_s s_\alpha^2 c_\alpha) + \frac{1}{2}\lambda_3 (v_s (c_\alpha^3 - 2 s_\alpha^2 c_\alpha) + v(s_\alpha^3 - 2 c_\alpha^2 s_\alpha)),$$

$$\lambda_{122} = 3(\lambda_1 v s_\alpha^2 c_\alpha - \lambda_2 v_s c_\alpha^2 s_\alpha) + \frac{1}{2}\lambda_3 (v_s (-s_\alpha^3 + 2 c_\alpha^2 s_\alpha) + v(c_\alpha^3 - 2 s_\alpha^2 c_\alpha)).$$

Using eqs (15)–(17), thermally averaged annihilation cross-section is calculated as

$$\langle \sigma v \rangle = \frac{1}{8 m^4 T_F K_2^2(m/T_F)} \times \int_{4m^2}^{\infty} ds\, \sigma(s)(s-4m^2)\sqrt{s}\, K_1\left(\frac{\sqrt{s}}{T_F}\right), \quad (18)$$

where K_i, $i = 1, 2$ are modified Bessel functions. Relic abundance for dark matter is then calculated by solving eqs (12)–(14), and using eq. (18) we calculate the relic density of the dark matter candidate.

5. Results

In this section, we present the results for the hidden fermionic dark matter candidate. We constrain the model parameter space using bounds from vacuum stability conditions 5 and bounds from LHC discussed earlier in §3 ($R_1 > 0.8$ [28] and $\mathrm{Br}^1_{\mathrm{inv}} < 0.2$ [29]). We then solve the Boltzmann equation for dark matter following eqs (12)–(18) in order to satisfy relic density for dark matter given by Planck (eq. (11)). We assume two different cases of h_2 mass with $m_2 = 100$ GeV and 110 GeV for non-SM scalar and h_1 to be the SM-like scalar having 125 GeV mass. We also consider two different values of VEV for dark Higgs doublet namely $v_s = 246$ GeV and 500 GeV. Using the model parameter space constrained by the above-mentioned conditions (vacuum stability, collider physics, dark matter relic density etc.) we test the viability of this fermionic dark matter candidate from direct and indirect detection results for dark matter.

5.1 *Direct detection*

Direct detection of dark matter is performed by different dark matter direct search experiments such as LUX [24], XENON100 [31], CDMS [32–34] etc. These dark matter experiments search for the collision of dark matter with the nucleus of the target or the detector material. The target nucleus of the detector material can undergo elastic scattering with dark matter particle. Dark matter direct search experiments measure the recoil energy of the target nuclei due to such elastic scattering and provide bound on the dark matter–nucleon direct detection cross-section. Depending on the initial spin of the detector nucleus, the scattering of the detector nucleus with DM can be either spin-independent or dependent. The spin-independent dark matter–nucleon scattering cross-section in the present model is given as [35]

$$\sigma_{\mathrm{SI}} = \frac{\sin^2 2\alpha}{4\pi} \frac{m^2}{v_s^2} m_r^2 \left(\frac{1}{m_1^2} - \frac{1}{m_2^2}\right)^2 \lambda_p^2, \quad (19)$$

where

$$\lambda_p = \frac{m_p}{v}\left[\sum_q f_q + \frac{2}{9}\left(1 - \sum_q f_q\right)\right] \simeq 1.3 \times 10^{-3}. \quad (20)$$

In eq. (19), $m_r = m m_p/(m + m_p)$ denotes the reduced mass for the dark matter–nucleon system while f_q in eq. (20) is the nuclear form factor and m_p is the mass of the proton. Using eqs (19) and (20), we test whether the fermionic dark matter in the present model can satisfy the bounds from dark matter direct search experiments. In figure 1, we show the variation of dark matter mass with spin-independent dark matter–nucleus elastic scattering cross-section. It is to be noted that the available model parameter space shown in figure 1 satisfies all the bounds from vacuum stability, limits from LHC and dark matter relic abundance obtained from Planck. Plots in

the upper panel of figure 1 are for $m_2 = 100$ GeV while the lower panel is plotted for $m_2 = 110$ GeV. The regions shown in red and green (for both upper and lower panels of figure 1) correspond to the choice of VEV, $v_s = 246$ GeV and 500 GeV. Also shown in the plots of figure 1, the blue line is the upper bound on dark matter–nucleon elastic scattering cross-section obtained from LUX experiment which provides the most stringent bound on dark matter–nucleon spin-independent scattering cross-section ($\sigma_{\rm SI}$). Hence, the plots in figure 1 indicate that there remains a valid region of model parameter space which is consistent with the bounds from dark matter direct detection. Therefore, fermionic dark matter in the present framework can serve as a potential candidate for dark matter in the mass range 40–60 GeV.

5.2 *Indirect detection*

Indirect detection of dark matter is based on the search for the excess in γ-ray, neutrino, electron–positron flux etc. originated from the galactic centre and other heavenly astrophysical bodies such as Sun. Massive astrophysical objects like galactic centre (GC) or Sun can trap dark matter particles. Dark matter particles can lose energy via scattering and as their velocity becomes smaller than the escape velocity of these massive astrophysical bodies with enormous gravitational pull, they get trapped. These dark matter particles, when accumulated in a considerable amount at the core of Sun or galaxy, can annihilate into a pair of fermions which can produce excess of γ-ray flux, neutrino flux etc. Observation of any such excess from these astrophysical sites can then be assumed to be due to annihilation of dark matter at these sites. Recent study of Fermi-LAT data [36] for GC γ-ray flux from GC by Calore, Cholis and Weniger (CCW) [37] has reported an excess in GC γ-ray flux in the energy range 2–10 GeV. CCW performed a detailed analysis of Fermi-LAT GC γ-ray flux data with 60 galactic diffusion excess (GDE) models. The analysis of CCW shows that such an excess of γ-ray at GC can be explained by a dark matter candidate of mass $49^{+6.4}_{-5.4}$ GeV primarily annihilating into $b\bar{b}$ pair with $\langle\sigma v\rangle_{b\bar{b}} = 1.76^{+0.28}_{-0.27} \times 10^{-26}$ cm^3 s^{-1}. The analysis of GC γ-ray by CCW is performed using a Navarro, Frenk and White (NFW [38]) dark matter halo profile with $\gamma = 1.26$ and local DM density $\rho_\odot = 0.4$ GeV cm^{-3} when observed over a region of galactic latitude $|l| \leq 20°$ and longitude $|b| \leq 20°$ but excluding inner $|b| \leq 2°$ region to avoid uncertainty. In this work, we explore whether the present framework of fermionic dark matter can explain the observed excess in γ-ray from GC. Differential γ-ray flux that subtends a solid angle dΩ at the centre of galaxy in a certain region of interest (ROI) is given as

$$\frac{{\rm d}\Phi}{{\rm d}E{\rm d}\Omega} = \frac{1}{8\pi m_{\rm DM}^2} J \sum_f \langle\sigma v\rangle_f \frac{{\rm d}N_f}{{\rm d}E_\gamma}, \tag{21}$$

where ${\rm d}N_f/{\rm d}E_\gamma$ denotes the spectrum for dark matter annihilating into a specific channel f while the corresponding annihilation cross-section is denoted as $\langle\sigma v\rangle_f$. Factor J is the line of sight integral

$$J = \int_{\rm los} \rho^2(r(s,\theta)){\rm d}s, \tag{22}$$

where θ is the measure of angular aperture connecting direction of line of sight (l.o.s.) and line from Earth to GC. The factor J depends on the nature of halo profile $\rho(r)$. Following the work by CCW, we consider NFW halo profile with $\gamma = 1.2$

$$\rho(r) = \rho_0 \frac{(r/r_s)^{-\gamma}}{(1 + r/r_s)^{3-\gamma}}, \tag{23}$$

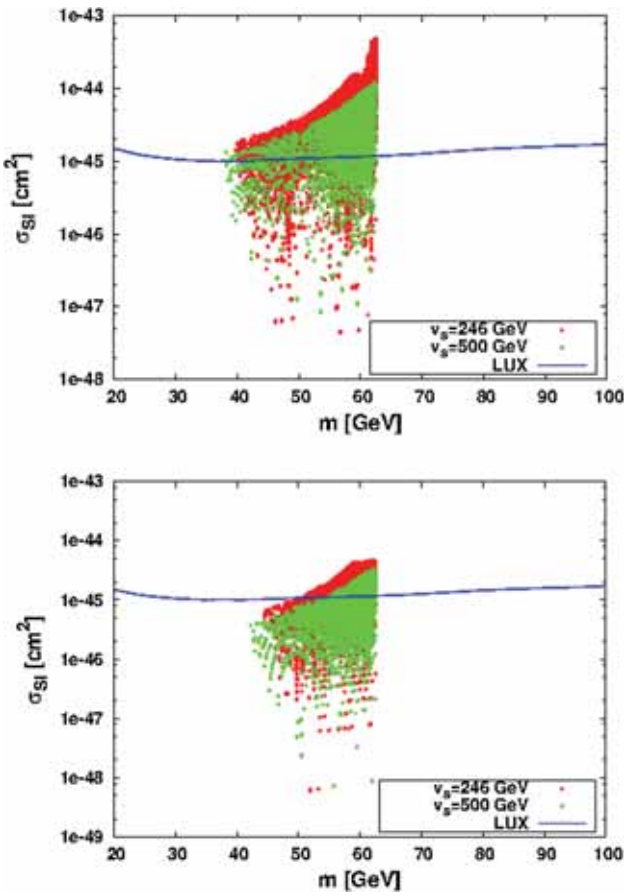

Figure 1. Valid $m-\sigma_{\rm SI}$ parameter space for hidden sector fermionic dark matter with $m_2 = 100$ GeV (upper panel) and 110 GeV (lower panel).

Table 1. Benchmark points consistent with model parameter space.

BP	m (GeV)	$\delta\,(10^{-3})$	$\gamma_2\,(10^{-6})$	$\sigma_{\rm SI}\,(10^{-46})\,({\rm cm}^2)$	$\langle\sigma v\rangle_{b\bar{b}}\,(10^{-26})\,({\rm cm}^3{\rm s}^{-1})$
1	50.0	−4.86	0.60	2.89	1.98
2	55.0	−5.85	0.43	1.13	1.90

Terms within braces denote the order of respective parameter value. BP1 corresponding to $m_2 \sim 100$ GeV and BP2 corresponding to $m_2 \sim 110$ GeV can be obtained using eq. (26).

where $r = \sqrt{r_\odot^2 + s^2 - 2r_\odot s\cos\theta}$, $r_s = 20$ kpc, ρ_0 denotes the DM density normalized with respect to the density of DM at the location of Sun $\rho_\odot = 0.4$ GeV cm^{-3} at $r_\odot = 8.5$ kpc which is the distance of the Sun from the Earth.

Since dark matter candidate in the present model is the fermion, the annihilation of dark matter into different channel is p wave process and varies as square of the velocity v of the annihilating dark matter particles. Velocity of dark matter particle varies as $\sim\sqrt{3/x}$, $x = m/T$. Hence, as the temperature (T) decreases, annihilation cross-section of the dark matter will also decrease as the average velocity $v \sim 10^{-3}$ at GC is very small to account for GC γ-ray excess. However, annihilation cross-section can be enhanced significantly via Breit–Wigner resonant enhancement [39,40]. From §5.1, it is observed that the allowed range of dark matter mass satisfying all the theoretical and experimental bounds is about 40–60 GeV. Dark matter with mass 40–60 GeV can annihilate dominantly into $b\bar{b}$ decay mode. Also, the required DM annihilation cross-section to explain the excess of γ-ray at GC is $\langle\sigma v\rangle_{b\bar{b}} \sim 1.76^{+0.28}_{-0.27} \times 10^{-26}\,{\rm cm}^3{\rm s}^{-1}$. Hence, in the present work we consider Breit–Wigner enhancement of $\langle\sigma v\rangle_{b\bar{b}}$ only. Breit–Wigner enhancement of dark matter annihilation cross-section can occur when dark matter mass is almost half of the mass of the mediator particle (h_2 in the present scenario with mass m_2). In this limit, the thermal-averaged DM annihilation cross-section can be written as

$$\langle\sigma v\rangle_{b\bar{b}} = \frac{4x}{K_2^2(x)}\int_0^{z_{\rm eff}} {\rm d}z\,\sigma(z)_{b\bar{b}}\,z\,\sqrt{1+z}\,K_1 \times(2\,x\,\sqrt{1+z}), \tag{24}$$

where centre of momentum energy s is expressed with a parameter z, i.e., $s = 4m^2(1+z)$. In eq. (24), $\sigma(z)_{b\bar{b}}$ is defined as

$$\sigma(z)_{b\bar{b}} = \frac{g_c}{4m^2}\,\frac{\sqrt{z}}{1+z}\,\frac{\left(1+z-(m_b^2/m^2)\right)^{3/2}}{[(z+\delta)^2+\gamma_2^2(1-\delta)^2]}, \tag{25}$$

which is expressed as a function of two parameters δ and γ_2 which are given as

$$m_2^2 = 4m^2(1-\delta) \quad \text{and} \quad \gamma_2 = \frac{\Gamma_2}{m_2}. \tag{26}$$

The factor g_c in eq. (25) is given as

$$g_c = \frac{N_c}{16\,\pi}\left(\frac{m\cos\alpha}{v_s}\,\frac{m_b\sin\alpha}{v}\right)^2. \tag{27}$$

Equation (26) indicates that $\delta < 0$ is a physical pole. As $m_{\rm DM} \sim m_2/2$, the term proportional to $1/[(s-m_2^2)^2 + m_2^2\Gamma_2^2]$ only will have significant contribution to the annihilation and other terms are neglected. It is observed that for a physical pole with $\delta < 0$, the integrand of eq. (26) becomes very small as z reaches $z_{\rm eff} \sim \max[4/x,\ 2|\delta|]$ [40,41]. Hence, using the above-mentioned Breit–Wigner enhancement technique we calculate the thermally-averaged annihilation cross-section $\langle\sigma v\rangle_{b\bar{b}}$ given in eq. (24) at GC. We consider two benchmark points respecting all the bounds (vacuum stability, LHC constraints, DM relic density, direct detection etc.) and calculate $\langle\sigma v\rangle_{b\bar{b}}$ for these benchmark points in order to explain the observed excess in γ-ray at GC obtained by Fermi-LAT. In table 1 we tabulate the benchmark points (BPs) in our model. From table 1 it can be easily concluded that Breit–Wigner resonance can enhance the dark matter annihilation cross-section significantly to achieve the required $\langle\sigma v\rangle_{b\bar{b}}$ in order to satisfy the excess of GC γ-ray observed by Fermi-LAT in agreement with analyses by CCW.

In figure 2, we show the comparison between the observed γ-ray excess at GC and the γ-ray flux obtained from benchmark points BP1 and BP2. The GC γ-ray flux for the benchmark points BP1 and BP2 are calculated using eqs (21)–(23) and Breit–Wigner resonance described in eqs (24)–(27). The spectrum ${\rm d}N_f/{\rm d}E_\gamma$ for any specific channel ($b\bar{b}$ in the present case) in order to calculate the γ-ray flux given in eq. (21) is obtained from Cirelli *et al* [42]. We have used the specific NFW halo profile with $\gamma = 1.2$ and calculated GC γ-ray flux for the ROI given by CCW [37], i.e., $|l| \le 20°$, $2° \le |b| \le 20°$. From figure 2 it can be concluded that the γ-ray flux obtained from benchmark points are in good

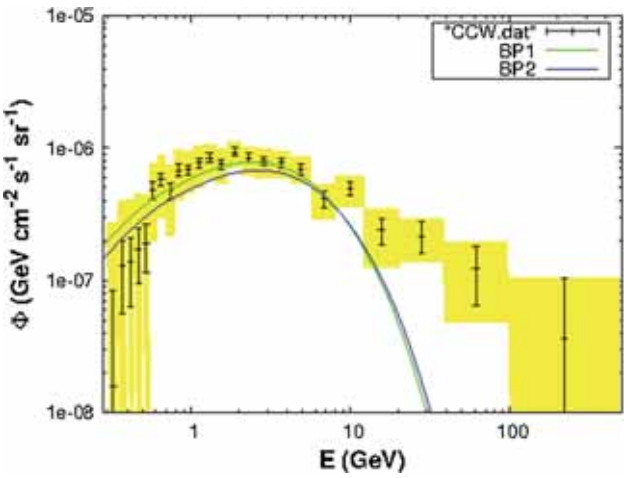

Figure 2. Comparison of γ-ray flux obtained from benchmark points with observed GC γ-ray results from CCW.

agreement with the analysis of GC γ-ray flux by CCW. Hence, the fermionic dark matter candidate in the present model can explain the observed γ-ray excess at GC.

6. Conclusion

We have proposed and explored a hidden sector model for dark matter. The dark sector follows a local $SU(2)_{\rm H}$ dark gauge symmetry and a $U(1)_{\rm H}$ global symmetry. The dark Higgs doublet does not have any $U(1)_{\rm H}$ global symmetry and is invariant under the local $SU(2)_{\rm H}$. However, fermions in the dark sector possess global $U(1)_{\rm H}$ symmetry. In order to avoid Witten anomaly, two generations of fermion doublets are added. After the spontaneous symmetry breaking, the dark Higgs doublet generates a VEV and generate masses of dark sector fermions and gauge bosons. The scalar in the dark sector mixes up with the scalar in SM sector resulting in two CP-even scalars. Among these two scalar bosons, one is assumed to be SM-like Higgs boson discovered at LHC (h_1) while the other is non-SM scalar (h_2). The lightest fermion in the dark sector can be a viable dark matter candidate. We have found that this fermion dark matter from hidden sector can indeed serve as a potential candidate for dark matter satisfying all the limits such as vacuum stability conditions, constraints on signal strength from LHC, dark matter relic abundance obtained from Planck and direct detection limits from LUX DM direct experiment. We further tested the viability of the hidden sector fermionic dark matter model with indirect detection signatures of dark matter with GC γ-ray excess data from Fermi-LAT. Our proposed fermionic dark matter candidate can also explain the observed excess in γ-ray from GC with Breit–Wigner enhancement of dark matter annihilation cross-section when the mass of dark matter is nearly half of the mass of non-SM scalar h_2.

Acknowledgements

One of the authors (D Majumdar) thanks the organizers of The First Workshop on Beyond Standard Model Physics (Pheno1) at IISER, Mohali, India for the invitation.

References

[1] Planck Collaboration: P A R Ade *et al*, *Astron. Astrophys.* **571**, A16 (2014)
[2] V Silveira and A Zee, *Phys. Lett. B* **161**, 136 (1985)
[3] A Hill and J J van der Bij, *Phys. Rev. D* **36**, 3463 (1987)
[4] E Ma, *Phys. Rev. D* **73**, 077301 (2006)
[5] L Lopez Honorez, E Nezri, J F Oliver and M H G Tytgat, *J. Cosmol. Astropart. Phys.* **0702**, 028 (2007)
[6] D Majumdar and A Ghosal, *Mod. Phys. Lett. A* **23**, 2011 (2008)
[7] M Aoki, S Kanemura and O Seto, *Phys. Lett. B* **685**, 313 (2010)
[8] A Bandyopadhyay, S Chakraborty, A Ghosal and D Majumdar, *J. High Energy Phys.* **1011**, 065 (2010)
[9] S Andreas, C Arina, T Hambye, F S Ling and M H G Tytgat, *Phys. Rev. D* **82**, 043522 (2010)
[10] Y Mambrini, *Phys. Rev. D* **84**, 115017 (2011)
[11] L Lopez Honorez and C E Yaguna, *J. Cosmol. Astropart. Phys.* **1101**, 002 (2011)
[12] D Borah and J M Cline, *Phys. Rev. D* **86**, 055001 (2012)
[13] Y Cai and T Li, *Phys. Rev. D* **88(11)**, 115004 (2013)
[14] A D Banik and D Majumdar, *Eur. Phys. J. C* **74(11)**, 3142 (2014)
[15] A D Banik and D Majumdar, *Phys. Lett. B* **743**, 420 (2015)
[16] P Ko and Y Tang, J. *Cosmol. Astropart. Phys.* **1501**, 023 (2015)
[17] M Kakizaki, A Santa and O Seto, arXiv:1609.06555 [hep-ph]
[18] T Hambye, *J. High Energy Phys.* **0901**, 028 (2009)
[19] D Hooper, *Phys. Rev. D* **91**, 035025 (2015)
[20] R Foot and S Vagnozzi, *Phys. Rev. D* **91**, 023512 (2015)
[21] A Biswas, *J. Phys. G* **43(5)**, 055201 (2016)
[22] C H Chen and T Nomura, arXiv:1501.07413 [hep-ph]
[23] K Ghorbani and H Ghorbani, arXiv:1504.03610 [hep-ph]
[24] LUX Collaboration: D S Akerib *et al*, *Phys. Rev. Lett.* **112**, 091303 (2014)
[25] E Witten, *Phys. Lett. B* **117**, 324 (1982)
[26] ATLAS Collaboration: G Aad *et al*, *Phys. Lett. B* **716**, 1 (2012)
[27] CMS Collaboration: S Chatrchyan *et al*, *Phys. Lett. B* **716**, 30 (2012)
[28] ATLAS Collaboration, ATLAS-CONF-2012-162
[29] G Belanger, B Dumont, U Ellwanger, J F Gunion and S Kraml, *Phys. Lett. B* **723**, 340 (2013)

[30] E W Kolb and M Turner, *The early Universe* (Westview Press, Boulder, 1990)
[31] XENON100 Collaboration: E Aprile *et al*, *Phys. Rev. Lett.* **109**, 181301 (2012)
[32] CDMS Collaboration: R Agnese *et al*, *Phys. Rev. D* **88**, 031104 (2013); *Phys. Rev. D* **88(5)**, 059901 (2013)
[33] CDMS Collaboration: R Agnese *et al*, *Phys. Rev. Lett.* **111(25)**, 251301 (2013)
[34] SuperCDMS Collaboration: R Agnese *et al*, arXiv:1504.05871 [hep-ex]
[35] L Lopez-Honorez, T Schwetz and J Zupan, *Phys. Lett. B* **716**, 179 (2012)
[36] Fermi Science Support Center, http://fermi.gsfc.nasa.gov/ssc/data/access/
Fermi-LAT Collaboration: W B Atwood *et al*, *Astrophys. J* **697**, 1071 (2009)
[37] F Calore, I Cholis and C Weniger, *J. Cosmol. Astropart. Phys.* **1503**, 038 (2015)
[38] J F Navarro, C S Frenk and S D M White, *Astrophys. J.* **462**, 563 (1996)
[39] M Ibe, H Murayama and T T Yanagida, *Phys. Rev. D* **79**, 095009 (2009)
[40] W L Guo and Y L Wu, *Phys. Rev. D* **79**, 055012 (2009)
[41] T Mondal and T Basak, *Phys. Lett. B* **744**, 208 (2015)
[42] M Cirelli *et al*, *J. Cosmol. Astropart. Phys.* **1103**, 051 (2011)